

## The Super-TIGER Instrument to Probe Galactic Cosmic Ray Origins

J.W. MITCHELL<sup>1</sup>, W.R. BINNS<sup>2</sup>, R.G. BOSE<sup>2</sup>, D.L. BRAUN<sup>2</sup>, E.R. CHRISTIAN<sup>1</sup>, W.M. DANIELS<sup>1</sup>, G.A. DE NOLFO<sup>1</sup>, P.F. DOWKONTT<sup>2</sup>, D.J. HAHNE<sup>1</sup>, T. HAMS<sup>1,a</sup>, M.H. ISRAEL<sup>2</sup>, J. KLEMIC<sup>3</sup>, A.W. LABRADOR<sup>3</sup>, J.T. LINK<sup>1,b</sup>, R.A. MEWALDT<sup>3</sup>, P. MOORE<sup>2</sup>, R.P. MURPHY<sup>2</sup>, M.A. OLEVITCH<sup>2</sup>, B.F. RAUCH<sup>2</sup>, F. SAN SEBASTIAN<sup>1</sup>, M. SASAKI<sup>1,c</sup>, G.E. SIMBURGER<sup>2</sup>, E.C. STONE<sup>3</sup>, C.J. WADDINGTON<sup>4</sup>, J.E. WARD<sup>2</sup>, AND M.E. WIEDENBECK<sup>5</sup>

<sup>1</sup> *NASA/Goddard Space Flight Center, Greenbelt, MD 20771 USA*

<sup>2</sup> *Washington University, St. Louis, MO 63130 USA*

<sup>3</sup> *California Institute of Technology, Pasadena, CA 91125 USA*

<sup>4</sup> *University of Minnesota, Minneapolis, MN 55455 USA*

<sup>5</sup> *Jet Propulsion Laboratory, California Institute of Technology, Pasadena, CA 91109 USA*

*John.W.Mitchell@nasa.gov*

DOI: 10.7529/ICRC2011/V06/1234

**Abstract:** Super-TIGER (Super Trans-Iron Galactic Element Recorder) is under construction for a 2012 long-duration balloon flight from Antarctica. This new instrument will measure the abundances of ultra-heavy elements ( $_{30}\text{Zn}$  and heavier), with individual element resolution, to provide sensitive tests of the emerging model of cosmic-ray origins in OB associations and models of the mechanism for selection of nuclei for acceleration. Super-TIGER builds on the techniques of TIGER, which produced the first well-resolved measurements of elemental abundances of the elements  $_{31}\text{Ga}$ ,  $_{32}\text{Ge}$ , and  $_{34}\text{Se}$ . Plastic scintillators together with acrylic and silica-aerogel Cherenkov detectors measure particle charge. Scintillating-fiber hodoscopes track particle trajectories. Super-TIGER has an active area of  $5.4 \text{ m}^2$ , divided into two independent modules. With reduced material thickness to decrease interactions, its effective geometry factor is  $\sim 6.4$  times larger than TIGER, allowing it to measure elements up to  $_{42}\text{Mo}$  with high statistical precision, and make exploratory measurements up to  $_{56}\text{Ba}$ . Super-TIGER will also accurately determine the energy spectra of the more abundant elements from  $_{10}\text{Ne}$  to  $_{29}\text{Cu}$  between 0.8 and 10 GeV/nucleon to test the hypothesis that microquasars or other sources could superpose spectral features. We will discuss the implications of Super-TIGER measurements for the study of cosmic-ray origins and will present the measurement technique, design, status, and expected performance, including numbers of events and resolution. Details of the hodoscopes, scintillators, and Cherenkov detectors will be given in other presentations at this conference.

**Keywords:** TIGER, Super-TIGER, Aerogel, GCR, Ultra-heavy GCR, refractory, volatile, OB association, microquasar

## 1 Introduction

The new Super-TIGER (Super Trans-Iron Galactic Element Recorder) long-duration balloon-borne instrument is in construction for its first Antarctic flight in 2012, with a second flight planned for 2014. Super-TIGER will measure the abundances of elements of atomic number  $30 \leq Z \leq 42$  with individual-element resolution and high statistical precision, and make exploratory measurements through  $Z=56$ . It will also measure with high statistical accuracy the energy spectra of the more abundant elements  $10 \leq Z \leq 30$  at energies from 0.8 GeV/nucleon to 10 GeV/nucleon, complementing the measurements expected from AMS. Super-TIGER builds on and improves the instrumental techniques developed for the Trans-Iron Galactic Element Recorder (TIGER) [1], successfully flown on two balloon flights from Antarctica in December of 2001 and 2003, yielding 50 days of data. Considering interaction losses in the instrument, Super-TIGER has an effective geometry

factor of  $2.5 \text{ m}^2\text{sr}$ , 6.4 times larger than TIGER. With about 60 days of Super-TIGER data expected from two Antarctic flights and lower levels of solar modulation anticipated the combined Super-TIGER/TIGER dataset will exceed present statistics by nearly an order of magnitude. These data will address important questions about galactic cosmic rays (GCR) including their origin, acceleration, and transport in the Galaxy.

TIGER produced the first well-resolved abundance measurements of  $_{31}\text{Ga}$ ,  $_{32}\text{Ge}$ , and  $_{34}\text{Se}$ , and an upper-limit on  $_{33}\text{As}$ . These data indicate nearly equal abundances of Ge and Ga and enrichment of the refractory elements by a factor of 3-4. TIGER also identified a mass dependent behavior for the refractory elements that is not explained by the model of Ellison et al.. Testing such a mass-dependent model requires a significant increase in statistics to quantify the abundances of the rare elements  $_{36}\text{Kr}$ ,  $_{37}\text{Rb}$ , and  $_{38}\text{Sr}$ . The TIGER results are shown in Figure 1, which gives the ratios as a function of atomic mass of Galactic cosmic ray

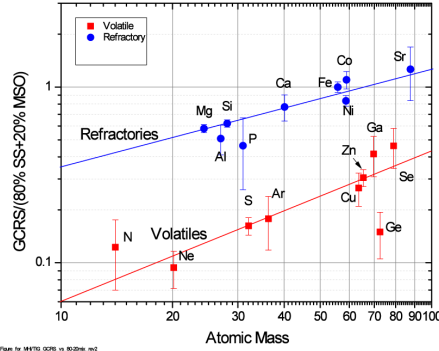


Figure 1: Ratio of GCRS abundances to a mixture of 80% SS and 20% MSO [1].

source (GCRS) abundances derived from TIGER data to a mixture of 80% solar system (SS) abundances and 20% massive star outflow (MSO) from Wolf-Rayet stars. The measured data are well ordered by this ratio, indicating that an admixture of MSO is required, although the precise mixture is not tightly constrained. Figure 1 indicates that refractory elements are preferentially accelerated and depend on mass ( $A$ ) as  $\sim A^{2/3}$  where the volatile elements are  $\sim A^1$ . The TIGER results support a model in which GCR nuclei originate from within OB associations [2, 3], regions within our Galaxy that contain young massive stars, and experience fractionation consistent with a preferential acceleration of elements found in interstellar grains (refractory) relative to those elements found in the interstellar gas (volatile). However, interpretation of the TIGER data is limited by the lack of statistical precision. The large increase in statistics enabled by Super-TIGER will provide a sensitive test of the hypothesis that GCR arise in OB associations.

Super-TIGER will also measure the energy spectra of the more abundant elements of  $10 \leq Z \leq 30$ . Together with measurements expected from AMS, this will provide a sensitive test of the hypothesis that microquasars or other discrete objects could contribute to the otherwise smooth energy spectra previously measured with less statistical accuracy.

## 2 Instrument

### 2.1 Instrument Description

Super-TIGER is designed to be the largest instrument that can be flown on a 1.11 mcm light balloon and achieve excellent charge resolution for  $Z \geq 30$  nuclei. Super-TIGER has an active area slightly more than 4 times TIGER. The instrument is divided into two independent modules, as shown in Figure 2, each approximately the width of TIGER and slightly more than twice as long. Each module has its own trigger and data acquisition computer. The modules

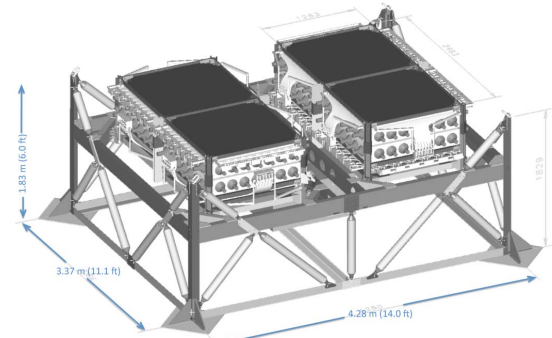


Figure 2: The fully integrated Super-TIGER payload showing the two instrument modules.

can be split into half-modules for recovery. The Super-TIGER configuration makes efficient use of the active area by measuring particles that "cross-over" between the active elements of the half-modules. Together with improvements to the mounting of the silica aerogel, this gives Super-TIGER an effective area greater than four times TIGER. In addition, the amount of material encountered by detected particles has been reduced, giving fewer interactions. From  $30 \leq Z \leq 42$  Super-TIGER will achieve a statistical precision of  $\sim 10\%$  or better for even-charges and  $\sim 20\%$  or better for odd-charges. The instrument techniques used for charge and energy measurement are identical to those successfully demonstrated on the smaller TIGER instrument with excellent Z-resolution ( $\sigma_Z = 0.23$ ) in the  $10 \leq Z \leq 38$  range.

A Super-TIGER module, shown in exploded view in Figure 3, consists of three layers of plastic scintillator [4] to measure charge, two Cherenkov counters [5] for velocity and charge measurements, and a scintillating-optical-fiber hodoscope [6] for trajectory determination. The scintillation layers (S1 & S2) that make the primary measurement of  $dE/dx$  are located just above the top hodoscope and below the Cherenkov detectors. The third scintillation counter (S3) is located just below the bottom fiber hodoscope. Placing the hodoscope between S2 and S3 decouples the two by preventing  $\delta$ -rays produced in S2 from reaching S3.

Particle charge is measured using  $dE/dx$  vs. Cherenkov and Cherenkov vs. Cherenkov techniques. These techniques are illustrated in Figure 4. The trajectory measured by the hodoscope, is used to correct for the incident angle and for instrument response maps. For low-energy events, below the aerogel (C0) threshold, the sum of two scintillator signals (S1+S2), with a small velocity correction from the acrylic (C1) signal, will be used to determine charge. For high-energy events, the C1 signal, with a small correction from the C0 signal, will be used to identify charge. The S3 signal is used to identify and reject particles interacting in the instrument. The Cherenkov counters also measure particle velocity (energy) and the use of acrylic radiators ( $n=1.5$ ) and aerogel radiators with two d-

ifferent refractive indices ( $n=1.043$  and  $1.025$ ) will allow Super-TIGER to measure the energy spectra of GCR nuclei from  $0.3$  GeV/nucleon to  $10$  GeV/nucleon. Each scin-

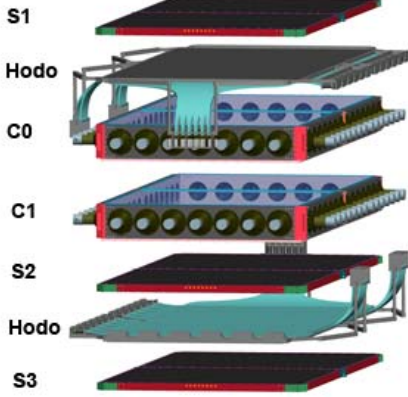


Figure 3: Exploded view of one Super-TIGER instrument module.

tillator layer contains two sheets of  $1.16\text{ m} \times 1.16\text{ m} \times 1\text{ cm}$  ELJEN EJ-208B plastic scintillator. The scintillation light produced in each sheet is read out with four EJ-280 waveshifter bars placed around the perimeter of each sheet, with a Hamamatsu R1924 PMT coupled to each end of each bar.

The Cherenkov light is collected using light integration volumes. The first counter (C0) uses aerogel radiators. Each aerogel Cherenkov module includes eight aerogel blocks, each approximately  $55\text{ cm} \times 55\text{ cm}$ . Three of the four half-modules will contain aerogel blocks of refractive index  $n = 1.043$  (12 blocks total), while one half-module will contain four blocks of index 1.025. These have thresholds of  $2.5$  GeV/nucleon and  $3.3$  GeV/nucleon, respectively. The second counter (C1) uses an acrylic radiator (with Bis-MSB waveshifter added) with an index of refraction of 1.5, corresponding to a threshold of  $0.3$  GeV/nucleon. In each module the acrylic radiator will consist of two  $1.16\text{ m} \times 1.16\text{ m}$  sheets.

Each of the hodoscope planes consists of two perpendicular layers of square scintillating fibers covering a fiducial area of  $2.4\text{ m} \times 1.16\text{ m}$ . Long axis fibers are  $1.4\text{ mm}$  square while short fibers are  $1\text{ mm}$ . The coded readout scheme developed for TIGER is used to limit the number of PMTs required. The fibers are formatted into tabs of 6 (long) or 8 (short) fibers, so the effective segmentation of the hodoscope is  $\sim 8\text{ mm}$ . Successive groups of 12 tabs at one end of each layer are combined into a segment viewed by a single PMT (Hamamatsu R-1924) to give coarse spatial resolution. The tabs on the opposite ends of the fibers are sequentially routed to PMTs, giving a finer spatial resolution that effectively acts as a vernier for the coarse tube readout. Each good event gives a hit at the fine end and one at the coarse end, thereby localizing the penetrating particle position to the  $8\text{ mm}$  width of a fine fiber tab. This gives a root-mean-square deviation in position of  $\sigma_{rms} = 8\text{ mm}/\sqrt{12} =$

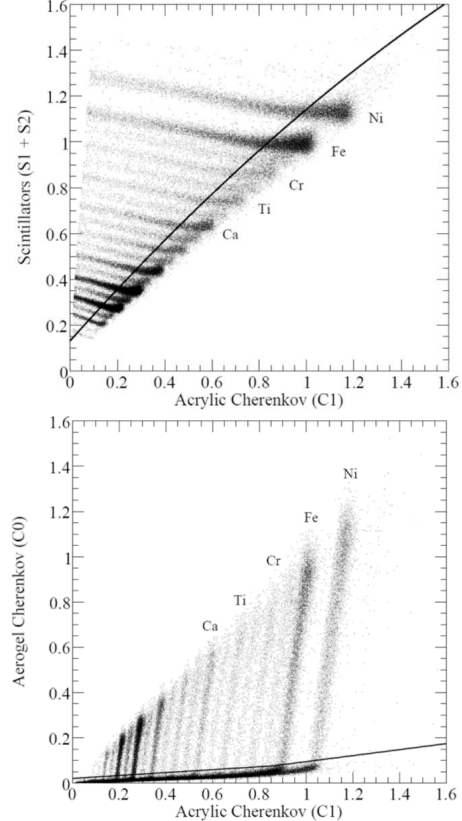


Figure 4: Data from TIGER illustrating the  $dE/dx$  vs. Cherenkov and Cherenkov vs. Cherenkov techniques for identifying charges.

$2.3\text{ mm}$ , which contributes only  $0.003$  charge units to the overall charge resolution for  $Z=40$  averaged over the effective opening angle of the instrument. The PMT signals are pulse-height analyzed so that large signals from nuclei can be readily distinguished from knock-on electrons. TIGER demonstrated that the coded fiber readout method is highly effective for high- $Z$  nuclei [7, 8, 1].

## 2.2 Expected Performance

Brookhaven accelerator tests of NE-114 plastic scintillator show a charge resolution of  $0.24$  c.u. for silver nuclei. The light output of the scintillators is characterized by a  $Z^{1.7}$  dependence over the charge range from  $^{31}\text{Ga}$  through  $^{47}\text{Ag}$  [9] and we expect good resolution in charge into the  $Z$  range above 50. In the analysis of our TIGER data, we successfully modeled scintillator saturation based on the detector response for iron and lower charges and extrapolated that to  $Z \geq 30$ . The Cherenkov counters will give even better charge resolution than the scintillators since they do not saturate and their signals have a  $Z^2$  dependence. In 1998 we calibrated an instrument complement, including the TIGER C0 (aerogel) and C1 (acrylic) Cherenkov counters, with a  $10.6$  GeV/nucleon gold beam at Brookhaven National Laboratory [10]. In this test we

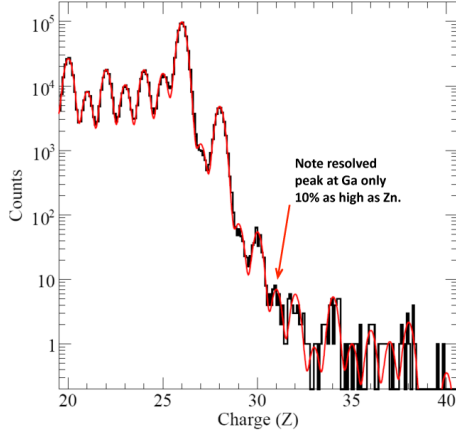


Figure 5: Charge histogram from the full TIGER dataset. The solid curve is a maximum likelihood fit.

obtained a resolution of 0.22 c.u. for gold nuclei in the acrylic counter, while in TIGER-2001 we achieved 0.23 cu resolution at iron for events above the aerogel Cherenkov threshold. For Super-TIGER, the light collection of various Cherenkov counter configurations and radiators was modeled using a GEANT4 Monte Carlo (MC), which uses the measured optical properties of the reflector, PMT quantum efficiency, absorption length, and Rayleigh scattering length in the Cherenkov radiator. Based on this simulation, we expect our charge resolution for high-energy nuclei will be essentially the same as TIGER. Figure 5 shows the charge histograms from the combined results of both TIGER flights (50 days) illustrating the excellent charge resolution ( $\sigma_Z = 0.23$  cu) we expect for Super-TIGER.

The Super-TIGER effective geometry factor (after interactions are removed) is  $2.5 \text{ m}^2\text{sr}$  compared to  $0.4 \text{ m}^2\text{sr}$  (calculated for  $^{34}\text{Se}$  nuclei), for TIGER. The anticipated level of solar modulation for flights in Dec. 2012 and 2014 compared to the levels during the TIGER flights in 2001 and 2003 gives an expected increase of a factor of 1.18 in numbers of particles. Additionally, assuming that Super-TIGER is flown twice for a total of 60 days compared to 50 days total flight time for TIGER gives an overall increase of nine for Super-TIGER over that of TIGER. Figure 6 shows a Monte Carlo simulation of the numbers of nuclei expected in two Super-TIGER flights assuming a total of 60 days at float and a charge resolution of 0.23 cu. There are clear peaks for each charge and we will be able to cleanly measure the abundances of all nuclei over the  $30 \leq Z \leq 42$  range.

### 2.3 Summary

Super-TIGER will measure the abundances of UH elements up to  $Z=42$  with exceptional statistical accuracy and make exploratory observations through  $Z=56$ . The combined Super-TIGER/TIGER data are expected to give nearly an order of magnitude increase in statistics. These

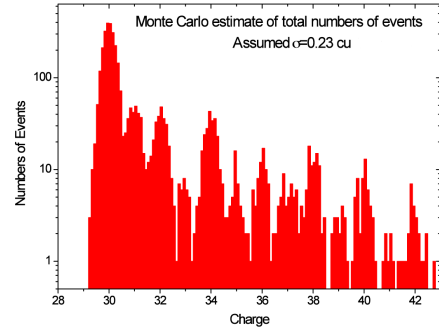


Figure 6: Monte-Carlo simulation of the numbers of events expected from two Super-TIGER flights.

data will probe all aspects of cosmic ray history from their origin, to acceleration, and finally to propagation.

### References

- [1] B.F. Rauch *et al.* *Astrophys J.*, 2009, **697** 2083–2088
- [2] J.C. Higdon & R. E. Lingenfelter *Astrophys J.*, 2003, **590**:822–832
- [3] W.R. Binns *et al.* *Astrophys J.*, 2005 , **634**:351–364
- [4] J.T. Link for the Super-TIGER collaboration, Proc. of 32nd ICRC (Beijing), 2011, O.G. 1.5, paper ID 0737
- [5] T. Hams for the Super-TIGER collaboration, Proc. of 32nd ICRC (Beijing), 2011, O.G. 1.5, paper ID 0831
- [6] J.E. Ward for the Super-TIGER collaboration, Proc. of 32nd ICRC (Beijing), 2011, O.G. 1.5, paper ID 0714
- [7] J.T. Link, 2003, PhD Thesis Washington University, St Louis, MO, USA.
- [8] B.F. Rauch, 2008, PhD Thesis Washington University, St Louis, MO, USA.
- [9] W.R. Binns *et al.* Proc. of 22nd ICRC (Dublin), 1991, **2**:511–514
- [10] J.R. Cummings *et al.* Proc. of 26th ICRC (Salt Lake), 1999, **2**:156–159
- [11] G.D. Westfall *et al.* *Physical Review C*, 1979, **19**:1309–1324

a. Also at: CRESST/University of MD Baltimore County, Baltimore, MD, 21250, USA.

b. Also at: CRESST/Universities Space Research Association, Columbia, MD, 21044, USA.

c. Also at: CRESST/University of MD College Park, MD, 20742, USA.